

## The Use of $\text{TiO}_2$ contaminated with Phosphorus and Potassium as a Support for $\text{V}_2\text{O}_5$ Catalysts in the Selective Oxidation of Toluene

S. Lars T. Andersson

*Department of Chemical Technology, Chemical Center, Lund Institute of Technology,  
P.O. Box 124, S-221 00 Lund, Sweden*

The structure of  $\text{V}_2\text{O}_5$ – $\text{TiO}_2$  catalysts, both of the supported type and the fused mixed oxide type, has been investigated by a variety of physicochemical techniques and correlated with their activity and selectivity in the oxidation of toluene. Special emphasis is put on the influence of phosphorus and potassium contaminants of commercial  $\text{TiO}_2$  preparations. These contaminants are mainly present in the  $\text{TiO}_2$  surface and prevent the formation of ideal monolayer catalysts. There are no results indicating V–P–O phase formation, but unselective potassium vanadate crystallites could be observed at a combination of high potassium and low vanadium concentrations. For fused catalysts of high vanadium contents, no such compound formation appears to occur. All preparations of low vanadium concentrations have a much lower activity in toluene oxidation than those of higher concentration containing bulk vanadium oxide crystallites. The selectivity for benzaldehyde could, however, be as high as for the most active catalyst prepared by the decomposition of  $\text{NH}_4\text{VO}_3$ . Selectivity for oxidative coupling products appears with the presence of vanadium oxide crystallites in catalysts with higher vanadium concentrations. Activity and selectivity data for the bulk  $\text{V}_2\text{O}_5$ – $\text{TiO}_2$  catalysts emphasizes the importance of defects and reduced phases.

Various metal oxides can be used as supports in the preparation of vanadium oxide catalysts for selective oxidation of hydrocarbons. The loading and type of support are important factors affecting the efficiency of the catalysts.<sup>1, 2</sup>  $\text{TiO}_2$  appears to be one of the best supports,<sup>3, 4</sup> and many studies have consequently been devoted to  $\text{V}_2\text{O}_5$ – $\text{TiO}_2$  catalysts, both of the supported<sup>2, 5–23</sup> and the mixed-oxide type,<sup>24–39</sup> as well as solid solutions.<sup>40–43</sup> From these it appears that in several cases maxima in selectivity and activity occur somewhere between *ca.* 2 and 50 mol %  $\text{V}_2\text{O}_5$ , probably influenced by the support surface area and a variation in the degree of reduction at steady state for different reactions and conditions.

Monolayer-type catalysts have been reported to give the best performance.<sup>6, 7, 10</sup> At these low vanadium concentrations differences in the support structure and contamination level may be of significance. The crystal modification of  $\text{TiO}_2$  in  $\text{V}_2\text{O}_5$ – $\text{TiO}_2$  catalysts is usually anatase, rutile or both. Several studies have been concerned with possible differences in the catalytic properties of supporting  $\text{V}_2\text{O}_5$  on the rutile or anatase modifications.<sup>44–48</sup> Thus it appears in several cases that anatase is to be preferred as support over rutile for the oxidation of ethylene,<sup>48</sup> *o*-xylene<sup>45</sup> and some alkylbenzenes<sup>44</sup> and for the  $\text{NO}$ – $\text{NH}_3$  reaction.<sup>15</sup> The main reason seems to be a better dispersion, giving a higher concentration of  $\text{V}=\text{O}$  species with anatase as support, but a higher turnover frequency is noted in some cases. In work on mixed-oxide systems,<sup>24–39</sup> however, correlations of selectivity and activity with  $\text{V}^{4+}$  concentration, the concentration of cation vacancies and the presence of lower oxides are reported.

It is well known that pure preparations of  $\text{TiO}_2$  are not easily made and therefore variations in the degree of contamination seem natural. In particular, some commercial preparations are known to contain phosphorus and potassium as contaminants.<sup>5-7, 12, 49, 50</sup> The negative influence of these at low vanadium concentrations has been shown,<sup>12, 49, 50</sup> and the effect of potassium is apparently larger than that of phosphorus.<sup>50</sup> The detailed manner in which these act in  $\text{V}_2\text{O}_5$ - $\text{TiO}_2$  catalysts is not known, although the effect of each in mixtures with  $\text{V}_2\text{O}_5$  alone is fairly well characterized. Thus in the V-P-O ternary system numerous phases exist, some of which show an increased selectivity for butene oxidation compared with  $\text{V}_2\text{O}_5$ .<sup>51, 52</sup> This is also the case for the V-K-O ternary system, but in *o*-xylene oxidation certain decomposition reactions produce  $\text{V}_6\text{O}_{13}$ .<sup>53</sup> For  $\text{V}_2\text{O}_5$  catalysts based on contaminated  $\text{TiO}_2$  the situation will be more complex, with a variety of possible phases in the  $\text{V}_2\text{O}_5$ - $\text{P}_2\text{O}_5$ - $\text{K}_2\text{O}$ - $\text{TiO}_2$  system, and even more if partial reduction is also considered. For  $\text{V}_2\text{O}_5$ - $\text{TiO}_2$  catalysts the addition of  $\text{P}_2\text{O}_5$  leads to increased acidity,<sup>54</sup> but the phase composition has not been studied. This is better understood for additions of  $\text{K}_2\text{O}$ , where potassium vanadates may form.<sup>55</sup> A catalyst prepared from contaminated  $\text{TiO}_2$  will perhaps have a different structure than one prepared from all four pure components directly.

In the present study results on catalysts based on contaminated rutile and also on contaminated anatase for low vanadium concentrations are discussed. Pure preparations will be used as the basis for future contributions. Thus, the catalytic oxidation of toluene has been studied and correlated with the structures and phase compositions of the catalysts as revealed by various experimental techniques.

## Experimental

### Catalyst Preparation

Fused catalysts were prepared by heating  $\text{V}_2\text{O}_5$  (Riedel-de-Haën) and  $\text{TiO}_2$  (anatase, Baker Chemical Co.) powders in quartz crucibles at 1150–1250 °C for 3 h. These catalysts will be called, for example, 10 $\text{V}_2\text{O}_5$ 90 $\text{TiO}_2$ , the figures showing the mol % of  $\text{V}_2\text{O}_5$  and  $\text{TiO}_2$  in the initial mixture. The 0.71–1.41 mm fractions were used in the catalytic measurements. A pure  $\text{V}_2\text{O}_5$  catalyst was also prepared by decomposition of  $\text{NH}_4\text{VO}_3$  in air at 500 °C for 8 h.  $\text{V}_2\text{O}_5$  supported on  $\text{TiO}_2$  (anatase or rutile) was prepared by impregnation with vanadyl acetylacetonate.<sup>56</sup> These catalysts will be referred to as *x* wt % V/anatase or V/rutile (RdH) or V/rutile (B). The rutile was prepared by heating anatase from Riedel-de-Haën (RdH) or Baker Chemical Co. (B) at 1150 °C for 3 h.  $\text{TiO}_2$  was suspended in benzene or ethanol solutions of vanadyl acetylacetonate overnight at room temperature. The solvent was thereafter evaporated at 80 °C and the samples were washed with pure solvent.

Preparations were performed both in air and in argon. The catalysts were calcined *in situ* in the catalytic reactor for 1 h at 400 or 500 °C. The final vanadium loadings were measured by atomic absorption spectroscopy.

### Activity Measurements

A conventional flow apparatus, described in detail elsewhere,<sup>57</sup> was used. Toluene was introduced by passing the flow through a series of saturators giving a toluene concentration of 1.28 vol % in air. After passing a preheater the flow entered the fixed-bed reactor (15 mm i.d.) loaded with 1–4 g of the catalyst. The isothermal operation of the reactor (400 ± 1 °C) was checked with thermocouples positioned at the bottom and upper ends of the bed. After passing through the reactor the flow was transported in heated tubes and divided in different streams for analysis of the partial oxidation products and carbon oxides. The analytical methods have been described in detail elsewhere.<sup>58</sup> Each experiment

was run for *ca.* 2–3 h and the data extrapolated back to zero time to obtain conversions and yields best representing the initial state of the catalysts. The reactor was operated with conversions between 0.2 and 8% and the rates were obtained from plots of conversion of yields against  $A/F$  ( $\text{m}^2 \text{ h mmol}^{-1}$ ), where  $A$  is the total surface area of the catalyst in  $\text{m}^2$  and  $F$  is the flow rate of toluene vapour in  $\text{mmol h}^{-1}$ .

### Atomic Absorption Spectroscopy

The concentration of vanadium in the supported catalysts were measured on a Varian AA-1275 atomic absorption spectroscope. The vanadium oxide on the support was dissolved in concentrated dichromate sulphuric acid, diluted to a suitable concentration and measured against standard vanadium solutions.

### Surface Area

Samples were outgassed at 300 °C for 1 h and measured on a differential B.E.T. apparatus suitable for low surface areas.<sup>59</sup> It was calibrated against an NBS standard of  $10.5 \text{ m}^2 \text{ g}^{-1}$ , checked on two other sets of B.E.T. apparatus. Reproducibility appeared to be within  $0.03 \text{ m}^2 \text{ g}^{-1}$ .

### X.R.D.

Philips X-ray diffraction instrument equipped with a PW 1310/01/01 generator and Cu  $K\alpha$  radiation was used.

### SEM

Scanning electron microscopic investigations were performed with an ISI-100A instrument equipped with a Princeton Gamma-Tech 1000 EDAX facility.

### PIXE

Particle-induced X-ray emission analysis performed at the facilities of the Department of Nuclear Physics using protons with an energy of 2.55 MeV from an electrostatic accelerator.

### E.S.R.

A Varian E-3 spectrometer was used for the e.s.r. studies. In the quantitative measurements a calibrated  $\text{V}_2\text{O}_5/\text{TiO}_2$  sample was run between each catalyst.

### ESCA

Measurements were performed on an AEI ES200B electron spectrometer equipped with an Al anode (1486.7 eV). The full width at half maximum of the Au  $4f_{7/2}$  core line was 1.8 eV. Sample charging was corrected using the hydrocarbon contamination C 1s line at 285.0 eV. For quantitative estimations, peak areas above a linear base line were measured with a planimeter. Owing to overlap with the O 1s  $K\alpha_{3,4}$  satellite, the V  $2p_{3/2}$  line could not be measured directly. Instead, the V  $2p_{3/2}$  + O 1s  $K\alpha_{3,4}$  intensity was measured. The V  $2p_{3/2}$  part was then calculated by subtracting the O 1s  $K\alpha_{3,4}$  part estimated from the O 1s  $K\alpha_{1,2}$  intensity with a weight factor measured for  $\text{TiO}_2$ . Calculations of theoretical  $I_{\text{V } 2p_{3/2}}/I_{\text{Ti } 2p_{3/2}}$  intensity ratios were done assuming monolayer formation up to a complete layer and thereafter with a second layer *etc.* The equations

**Table 1.** Surface areas and vanadium loading of V/rutile and V/anatase catalysts

catalyst	surface area $/\text{m}^2 \text{ g}^{-1}$	atomic absorption spectroscopy	
		$V/\text{mg m}^{-2}$	theoretical coverage <sup>a</sup>
0.20 wt % V/rutile (RdH)	0.33	6.1	7.2
0.024 wt % V/rutile (RdH)	0.33	0.7	0.9
0.096 wt % V/rutile (B)	0.45	2.3	2.7
0.43 wt % V/anatase (RdH)	8.61	0.5	0.6
0.88 wt % V/anatase (RdH)	8.61	1.0	1.2

<sup>a</sup> Units are 'number of monolayers' and calculated by dividing the number of V atoms per  $\text{m}^2$  by  $10^{19}$  since full monolayer coverage ( $\theta = 1$ ) is assumed for  $1 \times 10^{19} \text{ atom m}^{-2}$ .

used earlier for  $\text{V}/\text{Al}_2\text{O}_3$  catalysts were applied also here.<sup>60</sup> The data used were as follows: experimental sensitivity factors<sup>24</sup> for  $\text{O } 1s = 1$ ,  $\text{Ti } 2p_{3/2} = 1.37$  and  $\text{V } 2p_{3/2} = 2.17$  and literature data<sup>61</sup> for  $\text{K } 2p_{3/2} = 1$  and  $\text{P } 2p_{3/2} = 0.3$ , experimental intensity ratio for pure samples  $I_{\text{V } 2p_{3/2}}^\infty / I_{\text{Ti } 2p_{3/2}}^\infty = 1.58$ , monolayer thickness  $a = 2.34 \text{ \AA}$  and electron mean free paths for  $\text{V } 2p_{3/2}$  in  $\text{V}_2\text{O}_5$ ,  $\lambda_{\text{V}}(\text{V}_2\text{O}_5) = 25.3 \text{ \AA}$  and for  $\text{Ti } 2p_{3/2}$  in  $\text{V}_2\text{O}_5$ ,  $\lambda_{\text{Ti}}(\text{V}_2\text{O}_5) = 26.1 \text{ \AA}$  were calculated by the equation for inorganic samples.<sup>62</sup>

## Results and Discussion

### Characterization of the Catalysts

The  $\text{V}_2\text{O}_5/\text{TiO}_2$  catalysts prepared by fusing mixtures of  $\text{V}_2\text{O}_5$  and  $\text{TiO}_2$  powder have been characterized in detail earlier<sup>24, 25</sup> and the results for the fresh, unused catalysts are only cited here briefly. These were found to consist of two phases; an oxygen-deficient  $\text{V}_2\text{O}_5$  phase containing some  $\text{V}^{4+}$  and a rutile phase containing up to 6 atom %  $\text{V}^{4+}$ . At high  $\text{V}_2\text{O}_5$  concentrations the rutile particles were embedded in the  $\text{V}_2\text{O}_5$  phase. At low  $\text{V}_2\text{O}_5$  concentrations  $\text{VO}^{2+}$  ions were present on the surface of the rutile particles. The  $\text{V}^{4+}$  concentration in the  $\text{V}_2\text{O}_5$  phase varied with the  $\text{V}_2\text{O}_5$  concentration and showed a maximum at 50 mol %  $\text{V}_2\text{O}_5$ .

The 'monolayer'-type catalysts were characterized by B.E.T., X.r.d., SEM, e.s.r. and ESCA measurements in addition to a.a.s. and PIXE analyses. For all catalysts of the 'monolayer' type no peaks other than those due to the  $\text{TiO}_2$  phase could be detected in the X-ray diffractograms.

Table 1 shows the composition of these catalysts obtained by a.a.s. and PIXE analysis. The rutile samples were prepared from two different sources of  $\text{TiO}_2$ ; Riedel-de-Haën (RdH) and Baker Chemical Co. (B), and the anatase used as support was from Riedel-de-Haën. The specific surface areas of the rutile samples [(RdH) 0.33 and (B) 0.45  $\text{m}^2 \text{ g}^{-1}$ ] were much lower than that of the anatase samples (8.61  $\text{m}^2 \text{ g}^{-1}$ ). This was due to sintering of the  $\text{TiO}_2$  primary particles with an increase from 0.1 to 5–10  $\mu\text{m}$  during heat treatment. The vanadium loading of the catalysts was measured with a.a.s. and indicated theoretical monolayer coverages of 0.6 and 1.2 in the case of anatase as support. In the case of rutile as support the coverages were 0.9 and 7.2 for rutile (RdH) and 2.7 for rutile (B) (see table 1). The SEM studies revealed the presence of crystallites on the surface of the catalysts based on rutile as support, but not in the case of anatase (see plate 1).

In the 0.024 wt % V/rutile (RdH) catalyst [plate 1 (a)] the presence of crystallites is very sparse as compared with the 0.20 wt % V/rutile (RdH) catalyst [plates 1 (a)–(d)]. On the 0.096 wt % V/rutile (B) catalyst [plate 1 (e)] a few crystallite agglomerates were observed.

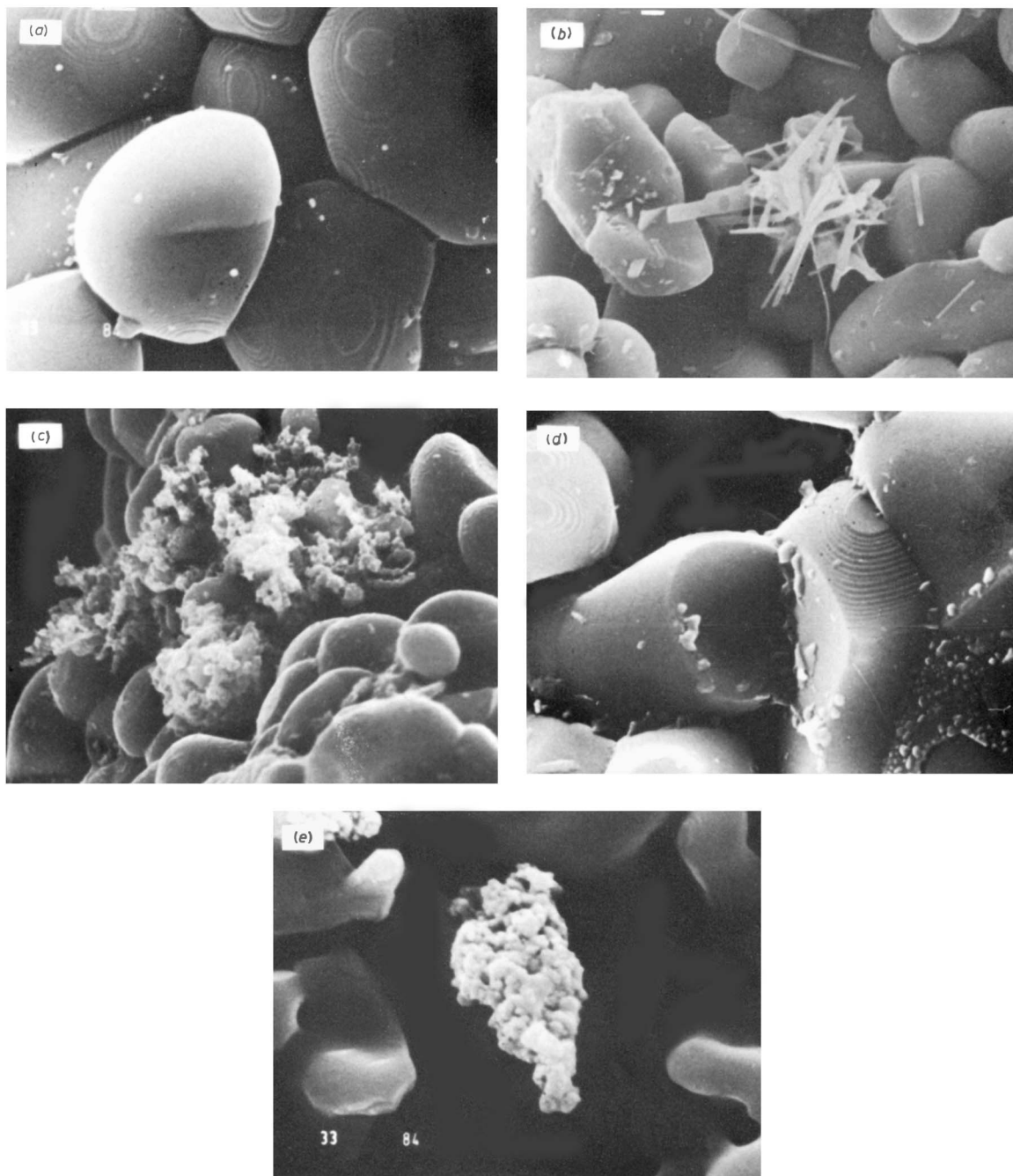


**Plate 1.** Micrographs of some used V/rutile catalysts. (The white line indicates a length of  $1\text{ }\mu\text{m}$ .)  
 (a) 0.024 wt % V/rutile (RdH), 10000  $\times$ ; (b) 0.20 wt % V/rutile (RdH), 5000  $\times$ ; (c) 0.20 wt % V/rutile (RdH), (different part), 5000  $\times$ ; (d) 0.20 wt % V/rutile (RdH), (different part), 10000  $\times$ ; (e) 0.096 wt % V/rutile (B), 15000  $\times$ .



**Table 2.** Concentration<sup>a</sup> of contaminations in V/rutile catalysts according to analysis by proton-induced X-ray emission (PIXE)

catalyst	PIXE								Ni, Cu, Zn, Sr, Zr, Nb
	P	S	Cl	K	Ca	Fe	Sb	W	
0.20 wt % V/rutile (RdH)	2100	510	420	1300	820	900	220	90	10–90
0.024 wt % V/rutile (RdH)	1900	390	380	1000	950	—	250	110	10–90
0.096 wt % V/rutile (B)	1000	440	380	— <sup>b</sup>	930	—	360	100	10–90

<sup>a</sup> Concentrations are given in ppm ( $\mu\text{g g}^{-1}$ ). <sup>b</sup> Detection limit, 145 ppm.

However, no plate-like crystallites or small particles (positioned at the interfaces between the  $\text{TiO}_2$  particles), as in the rutile (RdH) samples, could be observed. The different crystallite shapes in plates 1(b), (c) and (e) are interesting. The plate-like crystallites in (b) were identified by EDAX analysis to contain vanadium and potassium at a ratio of *ca.* 1.9. Phosphorus could not be detected by EDAX in the crystallites on any samples. The agglomerate of crystallites in (e) is very similar to parts of the agglomerate in (c). In this case EDAX analysis showed the presence of vanadium and potassium at a ratio of *ca.* 1.2. A large number of bronzes of the type  $\text{K}_x\text{V}_2\text{O}_5$  with  $x \leq 2$  exists.<sup>63</sup> By consulting the phase diagram<sup>64</sup> it is seen that there is a eutectic point at 390 °C and 40 mol %  $\text{K}_2\text{O}$ . This particular catalyst contains *ca.* 46 mol %  $\text{K}_2\text{O}$  by PIXE analysis, which is close to the composition of the eutectic point. It is thus feasible that during the catalytic reaction at 400 °C a melt is formed which, upon cooling, forms  $\text{K}_2\text{V}_8\text{O}_{21}$  and  $\text{K}_2\text{V}_2\text{O}_6$ . It has been suggested<sup>65</sup> that the  $\Psi$  bronze  $\text{K}_2\text{V}_8\text{O}_{20.8}$  is formed at 400 °C. The initial presence of vanadium in the tetravalent state may be crucial for the formation of these phases. The amorphous substance in plate 1(d) could not be identified definitely, but a weak signal for vanadium could perhaps identify the small particles as a vanadium phase. PIXE analysis (table 2) also identified iron impurities in this sample. Iron was only present in the 0.20 wt % V/rutile (RdH) sample and was in fact introduced by accident in this specific case. Concerning the other contaminants naturally occurring in  $\text{TiO}_2$  there is a difference between the Riedel-de-Haën and the Baker  $\text{TiO}_2$  samples. The rutile (RdH) sample contains *ca.* 2000 ppm P and 1000 ppm K, while the rutile (B) sample contains *ca.* 1000 ppm P and no K according to PIXE analysis.

Quantitative ESCA studies of these contaminations are presented in table 3. The bulk concentrations of these elements were <2000 ppm, which is close to the detection limit with the ESCA instrument used in these measurements. However, the K  $2p_{3/2}$  and P  $2p$  core lines were much stronger than expected, and almost of the same magnitude as the Ti  $2p_{3/2}$  core line. This fact strongly indicates the high surface enrichment and high dispersion of these contaminations. Consequently, seemingly low levels of contamination could affect the surface properties to an unexpectedly high degree. Concerning the other contaminants detected by PIXE, Ca was observed on all samples in the ESCA studies. The core-line intensity was, however, relatively much lower than for those of P and K. S and Cl could be observed only on fused catalysts, although the intensities were fairly low. These data would suggest that S, Cl and Ca are mainly present in the bulk and perhaps that S and Cl partly migrate to the surface upon heating to high temperatures. Such aspects have been considered earlier for chloride anions.<sup>66</sup> The high concentration of P in the surface may be due to a reaction in which phosphate anions are substituted for OH groups.<sup>66, 67</sup> The P  $2p$  and K  $2p_{3/2}$  binding energies of 133 and 292 eV, respectively, are consistent with their presence in an oxidized form. Potassium cations

**Table 3.** Vanadium, potassium and phosphorus concentrations in V/rutile, V/anatase and  $\text{V}_2\text{O}_5/\text{TiO}_2$  fused catalysts according to analysis by ESCA

catalyst	V/Ti	K/Ti	P/Ti	surface area /m <sup>2</sup> g <sup>-1</sup>
0.43 wt % V/anatase (RdH)	0.084	0.13	0.13	8.61
0.88 wt % V/anatase (RdH)	0.12	0.15	0.13	8.61
rutile (RdH)	—	0.41	0.34	0.33
0.024 wt % V/rutile (RdH)	0.16	0.45	0.39	0.33
0.20 wt % V/rutile (RdH)	0.40	0.40	0.29	0.33
0.096 wt % V/rutile (B)	0.17	0.21	0.38	0.45
10V <sub>2</sub> O <sub>5</sub> 90TiO <sub>2</sub>	1.8	0.57	0.49	0.07
30V <sub>2</sub> O <sub>5</sub> 70TiO <sub>2</sub>	4.1	0.44	0.61	0.13
50V <sub>2</sub> O <sub>5</sub> 50TiO <sub>2</sub>	5.7	0.46	0.54	0.22
70V <sub>2</sub> O <sub>5</sub> 30TiO <sub>2</sub>	6.1	0.62	0.97	0.19
90V <sub>2</sub> O <sub>5</sub> 10TiO <sub>2</sub>	22.0	0.55	1.17	0.19
100V <sub>2</sub> O <sub>5</sub>	∞	0	0	0.19

could then be bonded to phosphate anions and to formerly Brønsted-acidic OH groups on the  $\text{TiO}_2$  surface after substituting the proton. The data in table 3 show that the K/Ti and P/Ti ratios are 2–3 times larger for rutile (RdH) than for anatase (RdH). This is probably due to a decrease in the surface area due to sintering of the  $\text{TiO}_2$  particles during preparation of the rutile phase. The K and P contaminants are apparently still present in the surface to a large extent and with a higher concentration per unit area. The increases in K/Ti and P/Ti are, however, not as high as the decrease in surface area. From phase diagrams<sup>68</sup> it appears that no compound formation occurs between  $\text{TiO}_2$  and  $\text{P}_2\text{O}_5$ , but there are several in the  $\text{TiO}_2/\text{K}_2\text{O}$  and the  $\text{K}_2\text{O}/\text{P}_2\text{O}_5$  systems. With the K/P ratios < 1 found here the composition would lie in the  $\text{TiO}_2\text{--P}_2\text{O}_5\text{--(KPO}_3)_3$  ternary diagram, a region which is not well known. It is possible that a melt in the  $\text{P}_2\text{O}_5\text{--(KPO}_3)_3$  system is formed which, upon solidification, gives  $\text{P}_2\text{O}_5$  and  $(\text{KPO}_3)_3$  or some other intermittent potassium phosphate. It is not known if these bulk phase diagrams are applicable to surface phases.

The sample 0.096 wt % V/rutile(B), which did not contain potassium according to PIXE analysis, did in fact contain some potassium in the surface according to ESCA measurements. There is clearly a very strong surface enrichment. One may expect that the variation in surface concentration will affect the capability of 'monolayer' formation on these substrates. The rutile (RdH) samples with high K/Ti and P/Ti ratios did mostly form crystallites (*vide infra*), while the anatase preparations with much lower surface concentrations (lower K/Ti and P/Ti) formed 'monolayer' or isolated species. It is suggested that the higher concentration favours the formation of potassium vanadates (*vide supra*). A lower concentration of OH groups able to react with the vanadium species on the rutile samples may also be of significance. This lower concentration of OH groups is thought to occur partly through blocking by surface impurities, but it is also known that high-temperature treatment stabilizes the surface and a lower degree of rehydroxylation results.<sup>66</sup> In all samples the potassium and phosphorus surface concentrations are higher than needed for monolayer formation, but there is no proofs that these species are not agglomerated to some extent, producing some free  $\text{TiO}_2$  surface. Irrespective of the form in which potassium and especially phosphorus is present on the  $\text{TiO}_2$  surface initially, these seem to be very stable considering the results for fused catalysts. From ESCA measurements on the latter it appears as the P 2p and K 2p<sub>3/2</sub> binding energies are not affected by the heat treatment. Also, the P/Ti and K/Ti ratios are fairly constant, indicating P and K to be confined to the rutile surface and an absence of compound

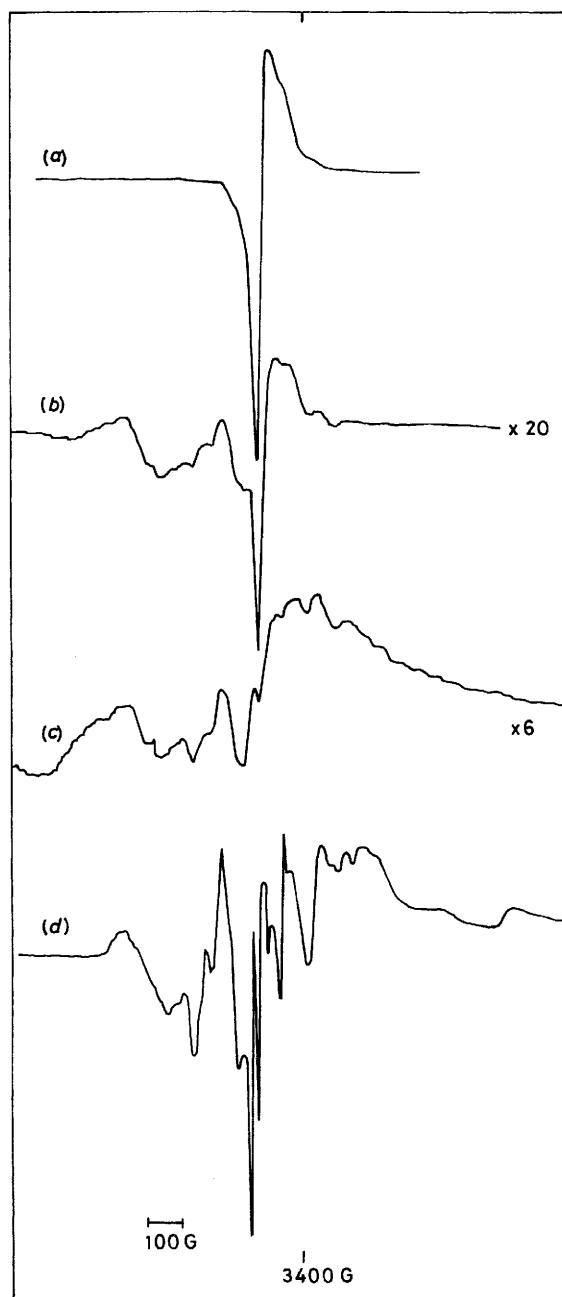


**Fig. 1.** E.s.r. spectra of some  $V_2O_5/TiO_2$  catalysts. (a) 0.20 wt % V/rutile (RdH), room temperature; (b) 0.024 wt % V/rutile (RdH), room temperature; (c) 0.096 wt % V/rutile (B), room temperature; (d) 0.43 and 0.88 wt % V/anatase, (77 K).



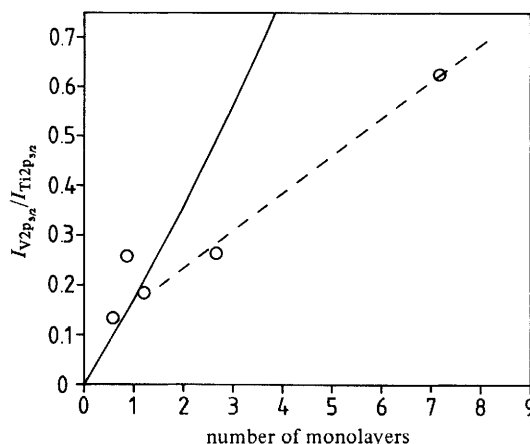


**Fig. 2.** Intensity ratio of the V  $2p_{3/2}$  to Ti  $2p_{3/2}$  core lines measured by ESCA as a function of the theoretical number of monolayers based on surface areas and a.a.s. analysis. (The solid line corresponds to  $I_{V2p_{3/2}}/I_{Ti2p_{3/2}}$  calculated for the ideal multilayer case as described in the Experimental section.)

formation with vanadium. Both P  $2p$  and K  $2p_{3/2}$  core lines thus decrease in intensity uniformly with the Ti  $2p_{3/2}$  core line as the V  $2p_{3/2}$  intensity increases with higher concentrations of  $\text{V}_2\text{O}_5$ . If a vanadium bronze or phosphate had formed one would expect these ratios to increase strongly. From the phase diagram<sup>64</sup> it is seen that with a  $\text{V}_2\text{O}_5$ – $\text{K}_2\text{O}$  composition close to  $\text{V}_2\text{O}_5$ , as in the fused catalysts,  $\text{V}_2\text{O}_5$  will crystallize first and thereafter  $\text{K}_2\text{V}_8\text{O}_{21}$ , which would then probably be on the surface. This contradicts the ESCA data. The observed small increases in the K/Ti and P/Ti ratios at increasing  $\text{V}_2\text{O}_5$  concentration are due to the longer escape depth of the K  $2p_{3/2}$  and P  $2p$  photoelectrons in comparison with Ti  $2p_{3/2}$  by 8 and 15%, respectively. No corrections were made to allow for such effects and the atom ratios calculated were obtained from the elemental sensitivity factors.

The e.s.r. studies gave additional information about the structure of these catalysts. The 0.20 wt % V/rutile (RdH) catalyst, which contained the higher number of crystallites, showed only a broad asymmetric e.s.r. signal [fig. 1 (a)] with a  $g$ -value of 1.97. It is probably due to  $\text{V}^{4+}$  present in the bronzes, also seen by SEM. There are only minor traces of hyperfine structure present, indicating the relatively low amount of surface  $\text{VO}^{2+}$  species. A catalyst based on the same support but with a lower vanadium loading [fig. 1 (b)] also showed a broad asymmetric line of the same origin superposed on an unresolved hyperfine structure. In this catalyst [0.024 wt % V/rutile (RdH)] the vanadium detected is present both as isolated  $\text{V}^{4+}$  or  $\text{VO}^{2+}$  on the rutile surface and in the vanadium bronze crystallites. The relative spin concentration of (a) to (b) is *ca.* 19:1, while the relative vanadium concentration is 8.3:1. For the 0.096 wt % V/rutile (B) catalyst the e.s.r. spectrum is mainly composed of an unresolved hyperfine structure [fig. 1 (c)]. A small peak is seen at the same position as for the broad signal [fig. 1 (a) and (b)], which indicates the relatively small number of crystallites. The major part of  $\text{V}^{4+}$  detected is thus present as isolated or perhaps rather slightly agglomerated  $\text{V}^{4+}$  or  $\text{VO}^{2+}$  species on the rutile surface. For this catalyst there is a better correspondence between the relative spin and vanadium concentrations [3.1 and 4, respectively, compared with 0.024 wt % V/rutile (RdH)]. A much better resolved hyperfine structure and with complete absence of crystallites was obtained for the 0.43 and 0.88 wt % V/anatase catalysts [fig. 1 (d)]. The spin concentration is the same for both samples, although the vanadium concentration

**Table 4.** Reaction rates and selectivities in the oxidation of toluene over V/TiO<sub>2</sub> (rutile) and V/TiO<sub>2</sub> (anatase) catalysts

catalyst	$r_{\text{toluene}}$ /mmol m <sup>-2</sup> h <sup>-1</sup>	selectivity (%)			$r_{\text{CO}_2}/r_{\text{CO}}$
		benzaldehyde	benzene	maleic anhydride	
rutile (B)	0.0089	15	—	—	4.6
anatase (RdH)	0.061	6	—	—	2.7
rutile (B)—6% V <sup>4+</sup> <sup>b</sup>	0.027	32	—	—	3.9
0.096 wt % V/rutile (B)	0.026	47 <sup>a</sup>	—	—	7
0.024 wt % V/rutile (RdH)	0.017	—	—	—	67
0.20 wt % V/rutile (RdH)	0.37	1	—	—	21
0.43 wt % V/anatase (RdH)	0.029	31	0.3	4	1.9
0.88 wt % V/anatase (RdH)	0.038	27	0.4	5	1.9

<sup>a</sup> At steady state 53% selectivity and  $r_{\text{toluene}} = 0.011 \text{ mmol h}^{-1} \text{ m}^{-2}$ . <sup>b</sup> Catalyst 10V<sub>2</sub>O<sub>5</sub>90TiO<sub>2</sub> treated with concentrated H<sub>2</sub>SO<sub>4</sub> to dissolve V<sub>2</sub>O<sub>5</sub>. Ca. 6 atom % V<sup>4+</sup> is left in the rutile phase.

differs. This could perhaps mean that the hyperfine structure represents stable VO<sup>2+</sup> species and that vanadium in excess of this amount is easily oxidized to V<sup>5+</sup> and thus not detected by e.s.r. The main differences between the rutile and anatase samples are that the VO<sup>2+</sup> species are fairly well dispersed on the anatase surface but less dispersed on the rutile surface. Furthermore, no crystallites are formed on anatase at low loadings, while on rutile crystallites are easily formed.

The ESCA spectra gave clearly visible V 2p<sub>3/2</sub> core lines of slightly higher magnitude than the closely lying O 1s Kα<sub>3,4</sub> satellite. The V 2p<sub>3/2</sub> binding energy around 516.7–517.1 eV is slightly higher than the value of 516.6 eV measured for pure V<sub>2</sub>O<sub>5</sub>. It is reasonable to assume that the main part of the vanadium giving rise to the ESCA spectra is present as V<sup>5+</sup>. The  $I_{\text{V } 2p_{3/2}}/I_{\text{Ti } 2p_{3/2}}$  intensity ratio as a function of the calculated number of monolayers is shown in fig. 2. For both catalysts with anatase as support with 0.6 and 1.2 monolayers (see table 1) the plots lie close to the theoretical line for the uniform multilayer model, which agrees with an absence of crystallite formation (*vide supra*). All three catalysts based on rutile as support, however, deviate from the calculated line. This is caused by the presence of vanadium bronze crystallites in these samples. The effect is especially apparent for the 0.20 wt % V/rutile (RdH) catalyst with the largest extent of crystallite formation. The measured  $I_{\text{V } 2p_{3/2}}/I_{\text{Ti } 2p_{3/2}}$  intensity ratio for this catalyst is much lower than expected if all the vanadium were present in a uniform layer. In this case a large portion of the vanadium in the crystallites is not contributing to the V 2p<sub>3/2</sub> core-line intensity in the ESCA spectrum, owing to the low electron escape depth.

### Catalytic Measurements

The catalytic vapour-phase oxidation of toluene is a complex reaction that may produce a large number of products with V<sub>2</sub>O<sub>5</sub> catalysts.<sup>57, 69, 70</sup> Three reaction routes are recognized; these are (i) oxidation in the side chain, (ii) oxidative coupling and (iii) oxidation in the aromatic nucleus. An important observation that deserves comments is that the oxidative coupling route is inhibited when the vanadium oxide is too well dispersed. The same effect was observed for V<sub>2</sub>O<sub>5</sub>/Al<sub>2</sub>O<sub>3</sub> catalysts,<sup>60</sup> and appears to be determined by the structure of the active phase (*vide infra*).

In table 4 the results on the monolayer (or rather supposed monolayer) catalysts are

shown. At the reaction conditions and conversion levels used these produce mainly benzaldehyde as the partially oxidized product. Both the selectivity for benzaldehyde and the rate of oxidation of toluene vary between these different catalysts. The lowest activity is observed for rutile (B), which also shows a low selectivity. In comparison anatase has a higher activity but a lower selectivity. These differences may be due to the different concentrations of impurities (*vide supra*), with a much lower surface concentration of phosphorus on rutile (B). Large  $\text{P}_2\text{O}_5$  additions render  $\text{TiO}_2$  acidic, but without activity in the oxidation reactions.<sup>54</sup> Supporting 0.96 wt % V on rutile (B) produces a catalyst with both higher activity and increased selectivity. This catalyst was found (*vide supra*) to contain very sparsely occurring crystallite agglomerates consisting of vanadium, probably in excess of that required to form the monolayer. Although containing an estimated 60% of the total vanadium content, the surface area of these agglomerates is negligible compared with that of the highly dispersed or monolayer vanadium. The selectivity, which increases to 53% at steady state, is similar to that found for the best  $\text{V}_2\text{O}_5$  catalysts, *i.e.* prepared by the decomposition of  $\text{NH}_4\text{VO}_3$ . The reaction rate per square metre is, however, much lower, only  $0.026 \text{ mmol g}^{-1} \text{ m}^{-2}$  compared with  $2.4 \text{ mmol g}^{-1} \text{ m}^{-2}$  for the  $\text{V}_2\text{O}_5$  catalyst. This low reaction rate is similar to that for the catalyst containing  $\text{V}^{4+}$  as a solid solution in the rutile structure [rutile (B) 6%  $\text{V}^{4+}$ ]. The selectivity is, however, much better. In addition to the production of benzaldehyde, with a selectivity of 51%, the pure  $\text{V}_2\text{O}_5$  catalyst produces other products in substantial quantities. These are due to further oxidation of the side-chain and to oxidative coupling of toluene and the further oxidation of these dinuclear species.<sup>70</sup> The main difference in the product selectivity is thus the presence or absence of the oxidative coupling route. We have found for  $\text{V}_2\text{O}_5/\text{Al}_2\text{O}_3$  catalysts<sup>60</sup> that it requires the presence of vanadium oxide crystallites, and does not proceed with agglomerates that are too small. Furthermore, studies on pure metal oxides<sup>57</sup> revealed the occurrence of coupling products for catalysts containing crystal planes with terminal oxygen. In conclusion, one may assume that the concentration and proximity of the  $\text{V}=\text{O}$  species are important. The much lower reaction rate of the monolayer catalyst may be due to two factors. When the  $\text{V}=\text{O}$  species occur isolated or in very small agglomerates the rate of the process may be determined simply by a shortage in the supply of oxide ions. Clearly, in large agglomerates or crystallites the replenishment of oxide ions, either by diffusion through the bulk or from nearby sites, should be largely facilitated. Also important seems to be the properties and configuration of the oxidant, *i.e.* the metal cation. In the case of isolated  $\text{V}=\text{O}$  species the transition from  $\text{V}^{5+}$  to  $\text{V}^{3+}$  is obtained on the release of the terminal oxygen. However, in the case of an agglomerate, with corner-shared octahedra, a simultaneous transition from corner- to edge-sharing octahedra will result in the formation of two  $\text{V}^{4+}$  on the release of a terminal oxygen. Calculations on  $\text{Mo}-\text{O}$  clusters have shown the facilitated release of oxygen when accompanied by crystallographic shear.<sup>71</sup> Consulting ionization potentials for gaseous ions the formation of two  $\text{V}^{4+}$  appears favourable, but in this case lattice and polarization effects are not considered. It is beneficial for the selectivity that these are more difficult to reoxidize. The smallest aggregate that can perform such a transition is thought to be formed by coupling two double-chain polyvanadate units (vanadium in a square pyramidal coordination), forming octahedral coordinated vanadium. This is similar to a small part of the  $\text{V}_2\text{O}_5$  structure. The mechanism discussed above does not exclude others working in parallel. For example, electron transfer to corner-shared octahedra has been suggested,<sup>52</sup> followed by a relaxation of only the intermittent double-bonded oxygen. In the case of a monolayer catalyst these mechanisms cannot be operating within a single layer of vanadium species. This would necessitate the involvement of the support surface cations. Consulting ionization potentials, however, suggests that there would be no difference between the formation of one  $\text{V}^{3+}$  or one  $\text{V}^{4+}$  plus one  $\text{Ti}^{3+}$ . The catalysts studied here were based on  $\text{TiO}_2$  with a high surface concentration of phosphorus, thought to be present as surface-bonded phosphate anions

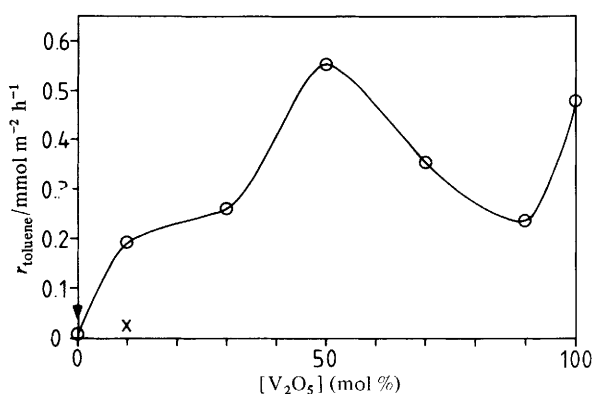


**Fig. 3.** Initial reaction rate (at zero time) of the oxidation of toluene over V<sub>2</sub>O<sub>5</sub>/TiO<sub>2</sub> (rutile) fused catalysts plotted against V<sub>2</sub>O<sub>5</sub> concentration. ○, Fresh catalyst; ×, catalyst treated with concentrated H<sub>2</sub>SO<sub>4</sub> to dissolve V<sub>2</sub>O<sub>5</sub>; ▼, TiO<sub>2</sub> (anatase).

(*vide supra*). Possibly, the vanadium units will be bonded on top of this layer in addition to the amount bonded on free TiO<sub>2</sub> surface. From ionization potentials it appears that the formation of two V<sup>4+</sup> or one V<sup>4+</sup> plus one P<sup>4+</sup> are energetically equivalent. This could also mean that V<sup>4+</sup> cations with a vacant adsorption site are turned into V<sup>5+</sup> cations with a vacant adsorption site by a similar electron transfer to a second nearby P<sup>5+</sup>. Thus the surface will be depleted of oxide ions and enriched in Lewis-acidic sites. These alone are not effective as oxidation catalysts, and such a catalyst should show a lower activity than a pure preparation. Indeed, the 0.43 and 0.88 wt % V/anatase preparations, containing a considerably lower amount of P and K contaminations, show a higher activity per unit area. The absence of crystallites and agglomerates in these preparations (*vide supra*) could perhaps explain the lower selectivity. That these preparations differ from the others is also seen in the formation of benzene and maleic anhydride and a lower  $r_{\text{CO}_2}/r_{\text{CO}}$  ratio. This ratio is suggested to reflect the CO oxidation activity (*vide infra*) and shows that these preparations are not as effective as CO oxidation catalysts. Since TiO<sub>2</sub> has a higher activity<sup>13</sup> in this reaction the data indicate, as is also suggested in the characterization studies, an improved coverage of the TiO<sub>2</sub> surface in the V/anatase preparations.

For the most contaminated catalysts, the 0.024 and 0.20 wt % V/rutile (RdH), there is almost no selectivity. In these catalysts with high potassium concentrations the vanadium is present only in the potassium vanadate crystallites (*vide supra*). These are probably of the Ψ phase composition that is completely unselective in *o*-xylene oxidation.<sup>65</sup> The 0.024 and 0.20 wt % V catalysts contain a vanadium surface concentration corresponding to a theoretical monolayer coverage of 0.9 and 7.2, respectively. The higher activity of the latter catalyst is due to the higher loading, in addition to the presence of iron oxide contamination. The different  $r_{\text{CO}_2}/r_{\text{CO}}$  ratio also indicates a difference in composition between these catalysts.

The impurities were observed to be strongly bonded to the surface (*vide supra*) and of negligible influence at vanadium concentrations > 10 mol % V<sub>2</sub>O<sub>5</sub>. Possibly a reduction at the V<sub>2</sub>O<sub>5</sub>/TiO<sub>2</sub> interface is required to obtain compound formation. The catalytic data for these catalysts are shown in fig. 3–6. The rate of oxidation of toluene (fig. 3) is much lower for TiO<sub>2</sub> than for any of the samples containing V<sub>2</sub>O<sub>5</sub>. There appears to be a difference between anatase and rutile, but it is not certain that it is due to a structural difference since there is a difference in the surface concentration of the contaminants (*vide supra*). The rutile sample with a solid solution of 6 atom % V<sup>4+</sup> shows an activity only slightly higher than for pure rutile. All preparations with a separate

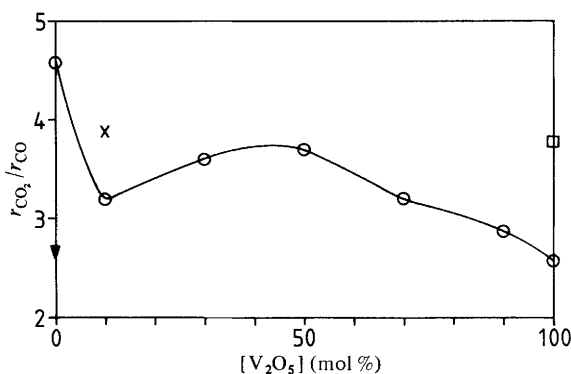


**Fig. 4.** Ratio ( $r_{\text{CO}_2}/r_{\text{CO}}$ ) of the rate of formation of  $\text{CO}_2$  to the rate of formation of  $\text{CO}$  in the oxidation of toluene over  $\text{V}_2\text{O}_5/\text{TiO}_2$  (rutile) fused catalysts plotted against the  $\text{V}_2\text{O}_5$  concentration.  $\circ$ , Fresh catalyst;  $\times$ , catalyst treated with concentrated  $\text{H}_2\text{SO}_4$  to dissolve  $\text{V}_2\text{O}_5$ ;  $\blacktriangledown$ ,  $\text{TiO}_2$  (anatase);  $\square$ ,  $\text{V}_2\text{O}_5$  prepared by decomposition of  $\text{NH}_4\text{VO}_3$ .

vanadium oxide phase show a much higher activity. The activity increases with  $\text{V}_2\text{O}_5$  concentration and has a maximum at *ca.* 50 mol %  $\text{V}_2\text{O}_5$ . This maximum may be connected with a similar maximum in the  $\text{V}^{4+}$  concentration of the  $\text{V}_2\text{O}_5$  phase in the fresh preparations, as measured by e.s.r. spectroscopy.<sup>25</sup> Preliminary experiments on slightly reduced catalysts revealed for all catalysts, except the 10 $\text{V}_2\text{O}_5$ 90 $\text{TiO}_2$  sample, a twofold or higher increase in activity. The activity of the slightly reduced 100 $\text{V}_2\text{O}_5$  catalyst had even increased to 2.6 mmol h<sup>-1</sup> m<sup>-2</sup>. This is similar to the value of 2.4 obtained for the  $\text{V}_2\text{O}_5$  catalyst prepared by decomposition of  $\text{NH}_4\text{VO}_3$ . These preparation techniques are known to introduce a high concentration of defects,<sup>25, 72</sup> and the above data support earlier findings on the superior activity of these, also reported for other reactions.<sup>20, 46, 47</sup> The reduction treatment is also known to produce other phases such as  $\text{V}_6\text{O}_{13}$  that are more active than  $\text{V}_2\text{O}_5$ .<sup>25, 27</sup> The fact that the reduced 10 $\text{V}_2\text{O}_5$ 90 $\text{TiO}_2$  catalyst gave a lower activity is due to two factors. It is known that lower  $\text{V}_2\text{O}_5$  concentrations lead to a higher degree of reduction under similar conditions.<sup>73</sup> For our catalyst highly dispersed  $\text{V}_2\text{O}_4$  is probably formed<sup>25</sup> and  $\text{V}_2\text{O}_4$  is known to be fairly inactive.<sup>74</sup> Fig. 4 shows the ratio of the rate of production of  $\text{CO}_2$  to  $\text{CO}$  ( $r_{\text{CO}_2}/r_{\text{CO}}$ ). It is thought to reflect the activity for oxidation of  $\text{CO}$ . It is then assumed that a major part of the  $\text{CO}$  is produced initially from the hydrocarbons and the major part of  $\text{CO}_2$  from  $\text{CO}$ . There are some similarities to the rate of oxidation of toluene (fig. 3). For example, the region of medium composition also shows a local maximum at *ca.* 50 mol %  $\text{V}_2\text{O}_5$  and a higher activity of the  $\text{V}_2\text{O}_5$  catalyst prepared by decomposition of  $\text{NH}_4\text{VO}_3$ . However, there are also dissimilarities in the higher activity of rutile and  $\text{V}^{4+}$  in rutile in the oxidation of  $\text{CO}$ . Some preliminary experiments indicate a lower activity for slightly reduced catalysts. These findings agree with results on  $\text{CO}$ -oxidation, and merely indicate the difference between the two reactants. Both the  $\text{CO}$ <sup>13, 72</sup> and toluene<sup>75, 76</sup> oxidation reactions are thought to occur *via* a redox mechanism, but with  $\text{CO}$  the reduction of the catalyst is the rate-determining step<sup>13</sup> whereas with toluene it is probably the initial H-abstraction.<sup>77</sup> In conclusion, these data support the above assumption that  $\text{CO}$  is initially formed in the oxidative decomposition reaction.

The oxidation of toluene over catalysts containing vanadium oxide mainly produces products *via* two different reaction paths; side-chain oxidation and oxidative coupling. The products formed under the conditions used in this study are for the first route mainly benzaldehyde, and for the second route anthraquinone, methyldiphenylmethanes (isomer distribution unknown) and 2- and 4-methyldiphenylmethanone in order of decreasing

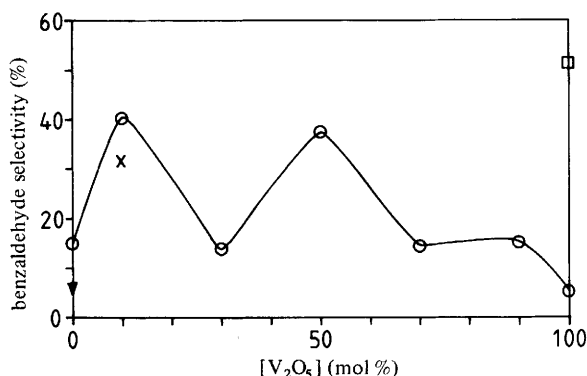


**Fig. 5.** Selectivity for benzaldehyde in the oxidation of toluene over V<sub>2</sub>O<sub>5</sub>/TiO<sub>2</sub> fused catalysts plotted against the V<sub>2</sub>O<sub>5</sub> concentration. ○, Fresh catalyst; ×, catalyst treated with concentrated H<sub>2</sub>SO<sub>4</sub> to dissolve V<sub>2</sub>O<sub>5</sub>; ▼, TiO<sub>2</sub> (anatase); □, V<sub>2</sub>O<sub>5</sub> prepared by decomposition of NH<sub>4</sub>VO<sub>3</sub>.

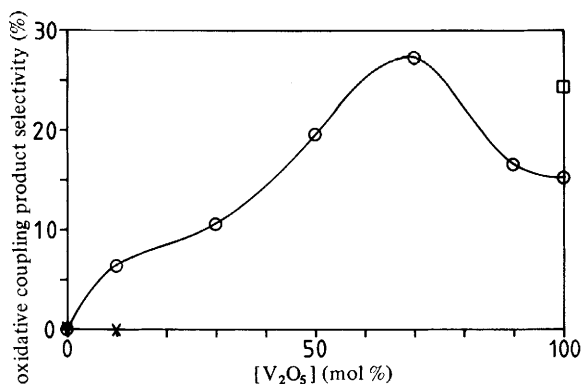


**Fig. 6.** Selectivity for oxidative coupling products in the oxidation of toluene over V<sub>2</sub>O<sub>5</sub>/TiO<sub>2</sub> fused catalysts plotted against the V<sub>2</sub>O<sub>5</sub> concentration. (The oxidative coupling products are anthraquinone, methylphenylmethane (isomer distribution not known), 2- and 4-methyldiphenylmethanone and phthalic anhydride). ○, Fresh catalyst; ×, catalyst treated with concentrated H<sub>2</sub>SO<sub>4</sub> to dissolve V<sub>2</sub>O<sub>5</sub>; ▼, TiO<sub>2</sub> (anatase); □, V<sub>2</sub>O<sub>5</sub> prepared by decomposition of NH<sub>4</sub>VO<sub>3</sub>.

importance. Fig. 5 shows the selectivity for benzaldehyde and fig. 6 the sum of selectivities for the products of the coupling route. It is seen that the selectivity for benzaldehyde is significantly lower for the fused V<sub>2</sub>O<sub>5</sub>/TiO<sub>2</sub> catalysts than for the V<sub>2</sub>O<sub>5</sub> catalyst prepared by decomposition of NH<sub>4</sub>VO<sub>3</sub>, probably owing to the higher defect concentration of the latter (*vide supra*). Except for the 10V<sub>2</sub>O<sub>5</sub>90TiO<sub>2</sub> catalyst, the dependence with a local maximum at 50 mol % V<sub>2</sub>O<sub>5</sub> correspond to the V<sup>4+</sup> concentration in the vanadium oxide phase, and once again the importance of defects is noted. The higher selectivity of 10V<sub>2</sub>O<sub>5</sub>90TiO<sub>2</sub> emphasizes its different nature, with a superior dispersion of V<sub>2</sub>O<sub>5</sub>. The lower V<sup>4+</sup> concentration in the V<sub>2</sub>O<sub>5</sub> phase of this sample suggests a superior selectivity by the small crystallites or agglomerates. Indeed, in the case of V<sub>6</sub>O<sub>13</sub> an amorphous surface phase showed a superior selectivity.<sup>78</sup> Preliminary experiments on reduced catalysts showed an increased selectivity of all catalysts except 10V<sub>2</sub>O<sub>5</sub>90TiO<sub>2</sub>, for which it decreased. These data are explained by the higher selectivity of catalysts with a higher defect concentration and the presence of reduced phases such as V<sub>6</sub>O<sub>13</sub>. The exception is due to over-reduction at low vanadium concentrations.

The selectivity for the oxidative coupling products (fig. 6) shows different behaviour.



Rutile and anatase have no selectivity and  $10\text{V}_2\text{O}_5/90\text{TiO}_2$  a low selectivity. These products are typical of  $\text{V}_2\text{O}_5$ ,<sup>57</sup> and the different nature of the crystallites at the higher dispersion in  $10\text{V}_2\text{O}_5/90\text{TiO}_2$  is emphasized. The overall behaviour with a maximum at approximately medium composition correlates with the  $\text{V}^{4+}$  concentration in the  $\text{V}_2\text{O}_5$  phase (*vide supra*). The selectivity at this maximum is similar to that of the  $\text{V}_2\text{O}_5$  catalyst prepared by decomposition of  $\text{NH}_4\text{VO}_3$ . Once again, partially reduced catalysts show a slight increase in selectivity.

The oxidative coupling products are typical of metal oxides containing double-bonded oxygen.<sup>57</sup> Isolated species are not active<sup>60</sup> and agglomeration of octahedra is a pre-requisite. The increased concentration of defects is favourable for a good catalytic performance of these agglomerates of octahedra. It is suggested that a specific coordination of octahedra is beneficial. Such could be obtained in the well annealed surface of the fused catalysts by (i) reduction, (ii) at a lower degree of crystallinity (as at low concentrations with higher dispersion) or (iii) as in the  $\text{V}_2\text{O}_5$  catalyst prepared by decomposition of  $\text{NH}_4\text{VO}_3$ . The need for the presence of both  $\text{V}^{4+}$  and  $\text{V}^{5+}$  in the catalysts was suggested to imply the cooperative action of a  $\text{V}^{4+}/\text{V}^{5+}$  couple in the activation of  $\text{O}_2$  and benzene in the formation of a bridge-bonded intermediate.<sup>79</sup> In the side-chain oxidation of toluene this mechanism is not valid and another active-site configuration and mode of action is suggested. Generally speaking,  $\text{V}^{4+}$  produces more weakly bonded oxide ions<sup>80</sup> and  $\text{V}^{5+}$  is beneficial as a stronger oxidant. The combination of these two effects indicates a more active catalyst. Selectivity for methyldiphenylmethanes seems to require a high concentration of terminal oxygen atoms. These are nucleophilic relative to the other oxygen species, and facilitate the initial rate-determining hydrogen abstraction. The reaction mechanisms have been discussed elsewhere.<sup>79</sup> An initial electron-transfer step with formation of a toluene radical cation could also be operative. However, the subsequent proton release produces the same species. The benzyl radicals formed couple to produce methyldiphenylmethanes or dimerize to produce bibenzyl. These species are then oxidized further. A high selectivity for coupling products is connected to a high concentration of benzyl radicals, and this then requires a high concentration of  $\text{V}^{5+}=\text{O}$  species. It also seems favourable for the coupling reaction if the molecule is not bonded to the surface *via* the substituent, but instead weakly bonded *via* the ring system. In the case of benzaldehyde formation, however, bond formation by the substituent should be favourable. Considering the criteria mentioned above, one could envisage a configuration of octahedra for an active site, but such a structure would be highly speculative considering the lack of direct experimental evidence.

## Conclusions

Phosphorus and potassium contaminants present in  $\text{TiO}_2$  are strongly confined to the surface. The lower surface area of rutile, prepared by heating anatase above the phase-transition temperature, results in a higher surface concentration of these species on rutile than on anatase. The contaminants are suggested to be present as surface-bonded phosphate and potassium ions. It is suggested that vanadia on such a surface is bonded by  $\text{V}-\text{O}-\text{Ti}$  as well as  $\text{V}-\text{O}-\text{P}$  bonds in quantities dependent on free  $\text{TiO}_2$  and the phosphate surface, respectively. The preparation of pure vanadia monolayer catalysts with such a surface is thus difficult. The reaction rate in the oxidation of toluene is not much increased following such a preparation compared with the support itself. Selectivity to benzaldehyde, however, is much improved. In preparations with high potassium surface concentrations, unselective potassium vanadate crystallites are formed.

For preparations with high  $\text{V}_2\text{O}_5$  concentrations ( $\geq 10 \text{ mol } \%$ ) no effects of the rutile surface contaminants are detected. The rate of toluene oxidation is much higher over these catalysts than over those of very low vanadium concentrations and they show a product pattern significant for vanadium oxide. The rate has a maximum around a

composition of 50 mol %  $V_2O_5$ , similar to the concentration of  $V^{4+}$  in the vanadium oxide phase as measured by e.s.r. spectroscopy. Preliminary experiments with reduced catalysts shows the superior activity of reduced phases, probably  $V_6O_{13}$ . At low vanadium concentrations ( $10V_2O_5/90TiO_2$ ), however, a lower activity is observed owing to the higher degree of reduction with the probable formation of  $V_2O_4$ . The selectivity for oxidative coupling products is also roughly proportional to the concentration of  $V^{4+}$  in the vanadium oxide phase. The selectivity for benzaldehyde shows similar behaviour, but with the important exception of a maximum selectivity for the catalyst  $10V_2O_5/90TiO_2$ . This difference underlines the effects of the active-site configuration. Thus there appear to be vanadium sites producing side-chain oxidation products and no oxidative coupling products, but we have not found the reversed case. Preliminary experiments show increased selectivities of the catalysts with reduction. The best catalyst identified so far is  $V_2O_5$  prepared by decomposition of  $NH_4VO_3$ , which is suggested to be due to a high concentration of defects with a specific configuration of octahedra.

I am grateful to Mrs B. Svensson for assistance in microscopic work and to Mr I. Aladjoff for surface-area measurements. The Swedish Board for Technical Development is acknowledged for financial support.

## References

- 1 See for example, Y. Murakami, M. Inomata, K. Mori, T. Ui, K. Suyzuyki, A. Miyamoto and T. Hattori, in *Preparation of Catalysts III*, ed. G. Poncelet, P. Grange and P. A. Jacobs (Elsevier Amsterdam, 1983), p. 531.
- 2 F. Roozeboom, M. C. Mittelmeijer-Hazeleger, J. A. Moulijn, J. Medema, V. H. J. de Beer and P. J. Gellings, *J. Phys. Chem.*, 1980, **84**, 2783.
- 3 W. Friedrichsen, *Chem. Ing. Techn.*, 1969, **41**, 967.
- 4 K. Hauße and H. Raveling, *Ber. Bunsenges. Phys. Chem.*, 1980, **84**, 912.
- 5 G. C. Bond, A. J. Sárkány and G. D. Parfitt, *J. Catal.*, 1979, **57**, 476.
- 6 G. C. Bond and K. Brückman, *Faraday Discuss. Chem. Soc.*, 1981, **72**, 235.
- 7 G. C. Bond and P. König, *J. Catal.*, 1982, **77**, 309.
- 8 A. Akimoto, M. Usami and E. Echigoya, *Bull. Chem. Soc. Jpn*, 1978, **51**, 2195.
- 9 Y. Nakagawa, T. Ono, H. Miyata and Y. Kubokawa, *J. Chem. Soc., Faraday Trans. 1*, 1983, **79**, 2929.
- 10 I. E. Wachs, R. Y. Saleh, S. S. Chan and C. C. Chersich, *Appl. Catal.*, 1985, **15**, 339.
- 11 I. E. Wachs, S. S. Chan and R. Y. Saleh, *J. Catal.*, 1985, **91**, 366.
- 12 A. J. Van Hengstum, J. G. Van Ommen, H. Bosch and P. J. Gellings, *Appl. Catal.*, 1983, **8**, 369.
- 13 F. Roozeboom, A. Jos van Dillen, J. W. Geus and P. J. Gellings, *Ind. Eng. Chem., Prod. Res. Dev.*, 1981, **20**, 304.
- 14 B. Grzybowska, Y. Barboux and J-P. Bonnelle, *J. Chem. Res. (M)*, 1981, 650.
- 15 M. Inomata, A. Miyamoto, T. Ui, K. Kobayashi and Y. Murakami, *Ind. Eng. Chem., Prod. Res. Dev.*, 1982, **21**, 424.
- 16 M. Inomata, A. Miyamoto and Y. Murakami, *J. Phys. Chem.*, 1981, **85**, 2372.
- 17 Y. Murakami, M. Inomata, A. Miyamoto and K. Mori, *Proc. 7th Int. Congr. Catal.*, ed. T. Seiyama and K. Tanabe (Elsevier, Amsterdam, 1981), p. 1344.
- 18 A. Miyamoto, K. Mori, M. Inomata and Y. Murakami, *Proc. 8th Int. Congr. Catal.*, (Verlag-Chemie, Weinheim, 1984), vol. IV, p. 285.
- 19 K. Mori, M. Inomata, A. Miyamoto and Y. Murakami, *J. Phys. Chem.*, 1983, **87**, 4560.
- 20 K. Mori, M. Inomata, A. Miyamoto and Y. Murakami, *J. Chem. Soc., Faraday Trans. 1*, 1984, **80**, 2655.
- 21 A. Miyato, Y. Nakagawa, T. Ono and Y. Kubokawa, *Chem. Lett.*, 1983, 1141.
- 22 R. Kozłowski, R. F. Pettifer and J. M. Thomas, *J. Phys. Chem.*, 1983, **87**, 5176.
- 23 K. O. Backhaus, R. Haase, U. Illgen, K. Jancke, J. Richter-Mendau, J. Scheve, I. Schulz and J. Vetter, *Ber. Bunsenges. Phys. Chem.*, 1983, **87**, 680.
- 24 S. L. T. Andersson, *J. Chem. Soc., Faraday Trans. 1*, 1979, **75**, 1356.
- 25 A. Andersson and S. L. T. Andersson, in *Solid State Chemistry in Catalysis*, *Am. Chem. Soc. Symp. Ser.* 279, ed. R. K. Grasselli and J. F. Brazdil, 1985, in press.
- 26 A. Andersson and S-T. Lundin, *J. Catal.* 1980, **65**, 9.
- 27 A. Andersson, *J. Catal.*, 1982, **76**, 144.
- 28 W. E. Slinkard and P. B. De Groot, *J. Catal.*, 1981, **68**, 423.
- 29 D. Kh. Sembaev, B. V. Suvorov, L. I. Saurambaeva and Kh. T. Suleimanov, *Kinet. Catal.*, 1979, **20**, 618.

- 30 D. Vanhove and M. Blanchard, *Bull. Soc. Chim. Fr.*, 1971, **9**, 3291.
- 31 M. Blanchard, G. Louguet, J. Rivasseau and J-C. Delgrange, *Bull. Soc. Chim. Fr.*, 1972, **8**, 3071.
- 32 D. J. Cole, C. F. Cullis and D. J. Hucknall, *J. Chem. Soc., Faraday Trans. 1*, 1976, **72**, 2185.
- 33 M. Ai, *Bull. Chem. Soc. Jpn*, 1976, **49**, 1328.
- 34 R. Grabowski, B. Grzybowska, J. Haber and J. Słoczyński, *React. Kinet. Catal. Lett.*, 1975, **2**, 81.
- 35 I. Gasior, M. Gasior, B. Grzybowska, R. Kozłowski and J. Słoczyński, *Bull. Acad. Pol. Sci., Ser. Sci. Chim.*, 1979, **27**, 829.
- 36 M. Gasior and B. Grzybowska, *Bull. Acad. Pol. Sci., Ser. Sci. Chim.*, 1979, **27**, 835.
- 37 B. Adamska, K. Brückman and B. Grzybowska, *Bull. Acad. Pol. Sci., Ser. Sci. Chim.*, 1978, **26**, 159.
- 38 R. Martino, L. Gambaro, E. Pereira and H. Thomas, *React. Kinet. Catal. Lett.*, 1983, **23**, 375.
- 39 M. Piechotta, I. Ebert and J. Scheve, *Z. Anorg. Allg. Chem.*, 1969, **368**, 10.
- 40 P. J. Pomonis and J. C. Vickerman, *J. Chem. Soc., Faraday Trans. 1*, 1981, **72**, 247.
- 41 P. J. Pomonis, *Proc. Vth Int. Symp. Heterogeneous Catal.*, ed. O. Shopov, A. Andreev, A. Palazov and L. Petrov (Bulgarian Acad. Sci., Sofia, 1983), vol. II, p. 45.
- 42 P. J. Pomonis and J. C. Vickerman, *J. Catal.*, 1984, **90**, 305.
- 43 M. R. Balasubramanian and K. S. De, *Ind. J. Chem.*, 1983, **22A**, 654.
- 44 M. Gasior, B. Grzybowska and M. Czerwenka, *Proc. Vth Int. Symp. Heterogeneous Catal.*, ed. O. Shopov, A. Andreev, A. Palazov and L. Petrov (Bulgarian Acad. Sci., Sofia, 1983), vol. I, p. 75.
- 45 M. Gasior, I. Gasior and B. Grzybowska, *Appl. Catal.*, 1984, **10**, 87.
- 46 K. Mori, M. Miura, A. Miyamoto and Y. Murakami, *J. Phys. Chem.*, 1984, **88**, 5232.
- 47 K. Mori, A. Miyamoto and Y. Murakami, *J. Phys. Chem.*, 1984, **88**, 2735.
- 48 K. Mori, A. Miyamoto and Y. Murakami, *J. Phys. Chem.*, 1984, **88**, 2741.
- 49 A. J. van Hengstum, J. G. van Ommen, H. Bosch and P. J. Gellings, *Proc. 8th Int. Congr. Catal.* (Verlag-Chernie, Weinheim, 1984), vol. IV, p. 297.
- 50 A. J. van Hengstum, J. Pranger, J. G. van Ommen and P. J. Gellings, *Appl. Catal.*, 1984, **11**, 317.
- 51 E. Bordes and P. Courtine, *J. Catal.*, 1979, **57**, 236.
- 52 M. Nakamura, K. Kawai and Y. Fujiwara, *J. Catal.*, 1974, **34**, 345.
- 53 M. Gasior, B. Grzybowska, J. Haber, T. Machej and J. Ziołkowski, *J. Catal.*, 1979, **58**, 15.
- 54 M. Ai, *Bull. Chem. Soc. Jpn*, 1977, **50**, 355.
- 55 A. A. Fotiev, A. P. Palkin, A. A. Soboleva and L. A. Perelyaeva, *Russ. J. Inorg. Chem.*, 1981, **26**, 576.
- 56 A. J. van Hengstum, J. C. van Ommen, H. Bosch and P. J. Gellings, *Appl. Catal.*, 1983, **5**, 207.
- 57 S. L. T. Andersson, in preparation.
- 58 S. L. T. Andersson, *J. Chromatogr. Sci.*, 1985, **23**, 17.
- 59 G. M. Bliznakov, I. V. Bakardjiev and E. M. Gocheva, *J. Catal.*, 1970, **18**, 260.
- 60 B. Jonson, B. Rebenstorf, R. Larsson, S. L. T. Andersson and S. T. Lundin, *J. Chem. Soc., Faraday Trans. 1*, 1986, **82**, 767.
- 61 W. J. Carter, G. K. Schweitzer and T. A. Carlson, *J. Electron. Spectrosc. Relat. Phenom.*, 1974, **5**, 827.
- 62 M. P. Seah and W. A. Dench, *Surf. Interface Anal.*, 1979, **1**, 2.
- 63 M. Pouchard and P. Hagenmuller, *Mater. Res. Bull.*, 1967, **2**, 801.
- 64 F. Holtzberg, A. Reisman, M. Berry and M. Berkenblit, *J. Am. Chem. Soc.*, 1956, **78**, 1538.
- 65 A. A. Fotiev, A. P. Palkin, A. A. Soboleva and L. A. Perelyaeva, *Russ. J. Inorg. Chem.*, 1981, **26**, 576.
- 66 G. D. Parfitt, *Progr. Surf. Membr. Sci.*, 1976, **11**, 181.
- 67 H. P. Boehm, *Adv. Catal.*, 1966, **16**, 179.
- 68 I. N. Belyaev and N. P. Sigida, *Zh. Neorg. Khim.*, 1958, **3**, 430.
- 69 J-E. Germain and R. Laugier, *Bull. Soc. Chim. Fr.*, 1971, **2**, 650.
- 70 S. L. T. Andersson, *J. Catal.*, in press.
- 71 E. Broclawik and J. Haber, *J. Catal.*, 1981, **72**, 379.
- 72 J. van den Berg, A. J. van Dillen, J. van den Meijden and J. W. Geus, in *Surface Properties of Non-Metal Catalysts*, ed. J. P. Bonnelle *et al.* (D. Reidel Publishing Company, Dordrecht, 1983), p. 493.
- 73 J. Haber, in *Mater. Sci. Monogr. 10*, Reactivity of Solids, ed. K. Dyrek, J. Haber and J. Nowotny (Elsevier, Amsterdam, 1982), vol. 1, p. 3.
- 74 A. Andersson and S. T. Lundin, *J. Catal.*, 1979, **58**, 383.
- 75 R. Trion, Th. van de Mond and P. J. van den Berg, *Delft. Progr. Rep.*, 1978, **3**, 263.
- 76 N. K. Nag, T. Fransen and P. Mars, *J. Catal.*, 1981, **68**, 77.
- 77 K. van der Wiele and P. J. van den Berg, *J. Catal.*, 1975, **39**, 437.
- 78 A. Andersson and J-O. Bovin, *Naturwissenschaften*, 1985, **72**, 209.
- 79 E. Broclawik, J. Haber and M. Witko, *J. Mol. Catal.*, 1984, **26**, 249.
- 80 G. Rasch, H. Bögel and C. Rein, *Z. Phys. Chem.*, 1978, **259**, 955.